





ORIGINAL ARTICLE OPEN ACCESS

Three-Dimensional Transjugular Intrahepatic Portosystemic Shunt Geometry Predicts Shunt Dysfunction

Carsten Meyer¹ | Markus Kimmann²  | Katharina Böhm³ | Sebastian Nowak¹ | Alba Maria Paar Pérez³ | Jörn Arne Meier² | Sara Noemi Reinartz Groba² | Juliana Gödiker²  | Frank Erhard Uschner² | Feras Sanoubara² | Johannes Chang³ | Jonel Trebicka^{2,4}  | Alois Martin Sprinkart¹ | Michael Praktijn^{2,3} 

¹Department of Diagnostic and Interventional Radiology, University of Bonn, Bonn, Germany | ²Department of Internal Medicine B, University of Münster, Münster, Germany | ³Department of Internal Medicine I, University of Bonn, Bonn, Germany | ⁴European Foundation for the Study of Chronic Liver Failure—EF CLIF, Barcelona, Spain

Correspondence: Michael Praktijn (michael.praktijn@ukmuenster.de)

Received: 12 December 2024 | **Revised:** 11 January 2025 | **Accepted:** 27 March 2025

Handling Editor: Palak J Trivedi

Funding: This work was supported by the Ernst-und-Berta Grimmke Foundation (Lfd.Nr. 5/19), the Else-Kröner Fresenius Foundation and the BONFOR research programme of the University of Bonn. Guarantor of article: PD Dr. Med. Michael Praktijn. Carsten Meyer, Markus Kimmann and Katharina Böhm should be considered joint first author. Alois Martin Sprinkart and Michael Praktijn should be considered joint senior author.

Keywords: cirrhosis | portal hypertension | transjugular intrahepatic portosystemic shunt

ABSTRACT

Background: Patients with decompensated cirrhosis are at risk of portal hypertension-related complications, such as refractory ascites or variceal bleeding. Transjugular intrahepatic portosystemic shunt (TIPS) insertion is the most effective treatment to reduce portal hypertension. However, patients are at risk for TIPS dysfunction.

Aims: We aimed to investigate the prognostic value of three-dimensional (3D) TIPS geometry in predicting TIPS dysfunction.

Methods: A total of 107 patients who underwent TIPS insertion between 2014 and 2019 and received a computed tomography (CT) scan after TIPS insertion during routine clinical practice were included. We used a semiautomated algorithm and multiplanar reconstructions of these CT scans to calculate parameters of 3D TIPS geometry. The primary outcome of this study was the development of TIPS dysfunction (defined as need for invasive TIPS revision). To identify predictors for the development of TIPS dysfunction, Cox regression analyses were performed with TIPS dysfunction as the endpoint.

Results: Thirty-two patients developed TIPS dysfunction and were compared to the dysfunction-free 75 patients. A larger distance from the cranial TIPS stent end to the vena cava inferior ($p < 0.001$, HR 1.061, 95% CI 1.030–1.093) and the maximum stent curvature ($p = 0.003$, HR 1.020, 95% CI 1.007–1.034) were significantly associated with TIPS dysfunction in a multivariate Cox regression analysis.

Conclusion: A more pronounced stent curvature and a longer cranial stent distance from the inferior vena cava were identified as independent predictors of TIPS dysfunction. Interventionalists should choose a more central and less curved TIPS tract during the TIPS procedure to reduce the risk of development of TIPS dysfunction.

Trial Registration: This retrospective monocentric study includes patients from the NEPTUN cohort (registered at Clinical Trials.gov; Identifier: NCT03628807).

Abbreviations: 2D, (two dimensional); 3D, (three dimensional); 95% CI, (95% confidence interval); CT, (computed tomography); CV, (central venous); HE, (hepatic encephalopathy); HR, (hazard ratio); INR, (international normalised ratio); IVC, (inferior vena cava); MELD, (model of end-stage liver disease); PSPG, (portosystemic pressure gradient); PTFE, (polytetrafluoroethylene); PV, (portal venous); TIPS, (transjugular intrahepatic portosystemic shunt); VCX, (VIATORR controlled expansion); VTS, (VIATORR TIPS).

This is an open access article under the terms of the [Creative Commons Attribution](https://creativecommons.org/licenses/by/4.0/) License, which permits use, distribution and reproduction in any medium, provided the original work is properly cited.

© 2025 The Author(s). *Alimentary Pharmacology & Therapeutics* published by John Wiley & Sons Ltd.

1 | Introduction

Liver cirrhosis with its severe complications caused by portal hypertension, such as variceal bleeding and refractory ascites, is a major healthcare burden. Patients with liver cirrhosis suffer from high rates of hospitalisation as well as increased morbidity and mortality [1].

Variceal bleeding and refractory ascites, as severe complications of portal hypertension, can be treated by implantation of a transjugular intrahepatic portosystemic shunt (TIPS). TIPS reduces the portosystemic pressure gradient by partially redirecting the portal venous blood flow to the inferior vena cava (IVC) [2]. In selected patients, TIPS can improve the outcome of patients with decompensated cirrhosis [3–7].

In the early era of bare metal stents, TIPS dysfunction was a major complication in up to 80% in 2 years [8, 9]. Technical advancements led to resolving several technical problems. However, the introduction of polytetrafluoroethylene (PTFE)-covered stents in the millenniums marked an important milestone, which reduced but did not abolish the problem of TIPS stent dysfunction [2, 10–12], which can have devastating clinical impacts such as variceal rebleeding or recurrent ascites.

TIPS dysfunction, including stenosis and occlusion, among other factors [13–16], seems to be influenced by the haemodynamic flow characteristics [17]. These are discussed to be influenced by the geometry and position of the TIPS stent. In the modern era of PTFE-covered TIPS stents, some studies suggested that characteristics of TIPS stent geometry and position, such as portal venous inflow angles and distance from the cranial stent end to the IVC, might predict TIPS dysfunction [18]. However, the data on especially two-dimensional (2D) assessed parameters are conflicting and do not seem to sufficiently reflect the complex portal venous anatomy [19, 20]. Data on three-dimensional (3D) assessed parameters are scarce because CT scan is not routinely performed after the TIPS procedure. Moreover, manual 3D reconstruction and the measurements of geometrical parameters are time-consuming procedures for healthcare professionals.

This study aimed to develop a semiautomated algorithm to assess 3D parameters and characteristics of TIPS geometry and to evaluate their predictive value for the development of TIPS dysfunction.

2 | Materials and Methods

2.1 | Study Population

This retrospective monocentric study includes patients from the NEPTUN cohort (registered at [ClinicalTrials.gov](https://clinicaltrials.gov/ct2/show/study/NCT03628807); Identifier: NCT03628807), who underwent the TIPS procedure between 2014 and 2019 and received a CT scan after TIPS insertion during routine clinical practice. Follow-up included evaluation of TIPS function using noninvasive imaging such as CT and ultrasound as well as clinical condition and standard biochemical blood analysis. Inclusion criteria were patient age of 18 or more and first-time implantation of a PTFE-covered TIPS stent

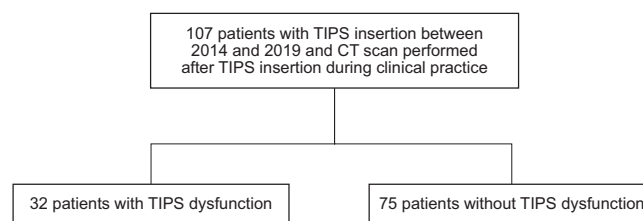


FIGURE 1 | Flow chart of study population.

for refractory ascites or variceal bleeding. Overall, 107 patients were eligible for this study (Figure 1). The primary endpoint was the development of TIPS dysfunction. TIPS dysfunction was suspected in the case of clinical signs like recurrence of ascites or variceal bleeding and followed by noninvasive tests to objectify TIPS dysfunction such as Doppler ultrasound with proof of reduction or nondetectability of flow in the stent and/or CT scan with signs of stent occlusion. Overall, the criteria used to define stent dysfunction were the same for all patients and based on the need for invasive revision of the TIPS. In the case of invasive visualisation with angiography without the need for invasive revision of the TIPS, we did not document the endpoint of TIPS dysfunction. Secondary endpoints were development of overt hepatic encephalopathy (HE) after TIPS in the entire cohort as well as detection of ascites at least 30 days after TIPS insertion in the subgroup of patients with refractory ascites as TIPS indication.

The ethical review board of the University Hospital of Bonn approved the study (positive ethical review board vote 038/20).

Written, informed consent was obtained from each patient included in the study.

The study protocol conforms to the ethical guidelines of the 1975 Declaration of Helsinki as reflected in a priori approval by the institution's human research committee.

2.2 | TIPS Procedure

An experienced team of hepatologists and radiologists performed the TIPS procedure to reduce the portosystemic pressure gradient (PSPG) under ultrasound and fluoroscopic guidance as previously described [21–23]. In summary, a tract was formed from the hepatic vein to the portal vein. The PSPG was measured before and after implantation of a PTFE-covered stent (W.L. Gore Medical). The types of stent grafts used in this study were the VIATORR TIPS (VTS) and the VIATORR controlled expansion (VCX) stent grafts.

The diameter of the stent was set at the interventionist's discretion according to PSPG measurement.

2.3 | Assessment of TIPS Geometry

First, multiplanar CT reconstructions were created using a proprietary programme (Intellispace; Philips Healthcare GmbH, Hamburg, Germany). Based on these MPRs, the evaluation was carried out by applying a dedicated software written in

MATLAB (Mathworks). A detailed explanation of the algorithm can be found in the Supporting Information 1.

In short, a venous path was generated starting from the beginning of the portal venous confluence through the TIPS to the IVC using multiplanar reconstructions orthogonal to the path, and different parameters of geometry were obtained (Figure 2).

- 3D cranial TIPS stent end (mm): distance of the cranial stent end to the IVC.
- 3D minimal stent diameter (mm): smallest diameter of the TIPS stent.
- 3D length of covered stent portion (mm): length from the beginning of the distal covered stent end to the end of the cranial covered stent end.
- 3D stent curvature (degrees/cm): Result of segmentation of the path within the TIPS stent into straight lines with gaps of 5 mm and angle measurements over 1 cm. The parameter describes the maximum change in direction between these sections within the entire stent. If the stent is straight, the value would be 0. Example: If the path makes

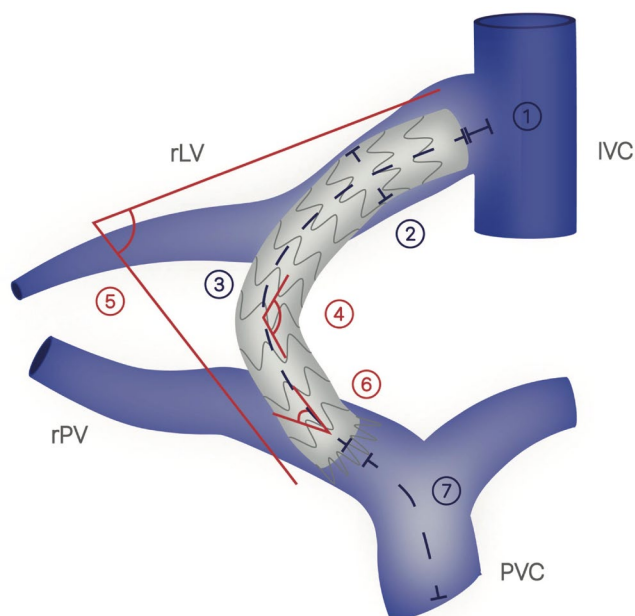


FIGURE 2 | Schematic illustration of the 3D TIPS geometry parameters. 3D cranial TIPS stent end (mm): Length from the cranial TIPS stent end in the liver vein to the IVC; 3D minimal stent diameter (mm): Smallest diameter in the entire TIPS stent; 3D length of covered stent portion (mm): Length from the beginning of the distal covered stent end to the end of the cranial covered stent end; 3D stent curvature (degrees/cm): Result of segmentation of the path within the TIPS stent into straight lines with gaps of 5 mm and angle measurements over 1 cm. The parameter describes the maximum change in direction between these sections within the entire stent; 3D angle between the covered stent ends (degrees): Angle between two straight lines orthogonal to the covered stent ends; 3D α angle (degrees): Angle formed between the beginning of the covered stent in the PV to the course of the PV; 3D confluence to TIPS stent (mm): Length from the beginning of the path to the beginning of the uncovered distal stent end.

a bend of 90° within one of the stent sections, the value would be 90.

- 3D angle between the covered stent ends (degrees): angle between two straight lines orthogonal to the covered stent ends.
- 3D α angle (degrees) angle between the caudal beginning of the covered stent in the PV and the course of the PV.
- 3D confluence to TIPS (mm): length from the beginning of the path to the beginning of the uncovered distal stent end.

2.4 | Statistical Analysis

SPSS (version 24, IBM, Armonk, NY, USA) was used to analyse all data. Descriptive statistics were performed for all variables. Categorical variables are presented in absolute cases and per cent, while continuous variables are presented as median with interquartile range. Nonparametric testing (Qui-square test for categorical variables, Mann–Whitney U test for continuous variables) was used to compare the groups with and without TIPS dysfunction. Uni- and multivariate Cox regression analysis with TIPS dysfunction as the endpoint was performed to identify predictors of TIPS dysfunction. To evaluate the relevance of the time from TIPS insertion to CT acquisition, an additional Cox regression analysis was performed, including the parameters that were significantly associated with TIPS dysfunction in the multivariate Cox regression analysis, as well as the time from TIPS insertion to CT acquisition. Furthermore, we performed an additional Cox regression analysis with overt HE as the endpoint, including the parameters that were significantly associated with TIPS dysfunction in the previous analysis. Additionally, a Cox regression analysis was performed in the subgroup of patients with refractory ascites as the indication for TIPS, with detection of ascites 30 days after TIPS insertion as the endpoint. All parameters with p -values <0.1 in the univariate analysis were considered potential risk factors and therefore included in the multivariate model. The multivariate Cox regression analysis was performed using forward stepwise logistic regression, excluding all parameters with p -values >0.1 . In case of missing parameters within the Cox regression model, the case was excluded for this particular analysis. p -Values below 0.05 were considered statistically significant.

3 | Results

3.1 | General Patient Characteristics at Baseline

This study included 107 patients; 57 (53.3%) patients were male. The median age was 58 (51–65). Most patients had alcohol-related liver cirrhosis ($n=63$; 58.9%). The main indications for TIPS were refractory ascites ($n=60$; 56.15%) and variceal bleeding ($n=37$, 34.6%). Eighty patients (74.8%) presented with ascites at the time of TIPS placement. In the entire cohort, 61 (57%) of patients received the VTS stent graft and 46 (43%) of patients received the VCX stent graft.

Overall, 32 patients developed TIPS dysfunction. The median times were 539 (127.75–985) days from TIPS procedure to TIPS

dysfunction, 337 (29–612) days from TIPS procedure to CT acquisition and 134 (4.75–505.5) days from CT acquisition to TIPS dysfunction. The TIPS dysfunction group had a median age of 58 (51–64) and included 15 (46.9%) men. The main indication for TIPS in the TIPS dysfunction group was refractory ascites ($n=21$; 65.6%), and the main aetiology of cirrhosis was alcohol related ($n=19$; 59.38%). In the dysfunction group, 20 (62.5%) received a VTS stent graft, while 12 (37.5%) received a VCX stent graft. The group without TIPS dysfunction had a median age of 58 (51–65) and included 42 ($n=56\%$) male patients; 41 (54.7%) of patients received a VTS stent graft and 34 (45.3%) received a VCX stent graft. Both groups were comparable in terms of general characteristics, medical history, scores, hepatic haemodynamics before and after TIPS and distribution of used stent grafts (VCX and VTS) (Table 1 and Table 2). Noteworthy, the median portosystemic pressure gradient (PSPG) before TIPS revision in the TIPS dysfunction group was 18 mmHg [13–25].

A total of 73 patients (68.2%) presented with overt HE after the TIPS procedure during the entire follow-up, while 57 patients (53.3%) presented with overt HE within 12 months after the TIPS procedure. The median time to overt HE in the entire cohort was 49 days. Interestingly, there were no significant differences regarding parameters of 3D TIPS geometry or procedure data between two groups (Table S1).

3.2 | 3D Assessment From CT Reconstruction

The median 3D stent curvature was 42.12 (36.47–50.37) degrees. The median angle between the covered stent ends was 81.60 (68.88–98.73) degrees, and the median length from the cranial TIPS stent end to the IVC was 9.99 (2.00–17.93) mm. The median length from the portal venous confluence to the caudal TIPS stent was 60.02 (48.02–77.04) mm, while the median length of the covered stent portion was 63.03 (55.01–72.00) mm. The median minimum stent diameter was 8.27 (7.71–9.01) mm and the median 3D α angle was 53.71 (40.64–64.92) degrees.

In the TIPS dysfunction group, the distance of the cranial TIPS stent end to the IVC (16.49 vs. 6.00; $p<0.001$) and the 3D stent curvature (47.21 vs. 40.68, $p=0.017$) were significantly larger compared to the dysfunction-free group. Moreover, the length of the covered stent portion was significantly shorter in the TIPS dysfunction group (55.45 vs. 66.02; $p=0.001$) (Table 2).

3.3 | Predictors of TIPS Dysfunction

An univariate Cox regression analysis with TIPS dysfunction as the endpoint was performed. The 3D stent curvature ($p=0.002$, HR 1.019, 95% CI 1.007–1.032) and the 3D cranial TIPS stent end ($p<0.001$, HR 1.057, 95% CI 1.026–1.090) were significantly associated with TIPS dysfunction in the univariate approach. The 3D length of the covered stent portion ($p=0.066$, HR 0.967, 95% CI 0.934–1.002) closely failed to reach statistical significance and was also included in the multivariate analysis. Regarding procedure data, the nominal stent length ($p=0.062$, HR 0.741, 95% CI 0.541–1.016) as well as the status of underdilation of the TIPS ($p=0.069$, HR 0.429, 95% CI 0.173–1.069) were also included in the multivariate analysis. Of note, data on haemodynamics like

central venous (CV) pressure, portal venous (PV) pressure and PSPG before and after TIPS insertion were not associated with the development of TIPS dysfunction.

In the multivariate analysis, only the 3D stent curvature ($p=0.003$, HR 1.020, 95% CI 1.007–1.034) and the 3D cranial TIPS stent end ($p<0.001$, HR 1.061, 95% CI 1.030–1.093) were significantly associated with the development of TIPS dysfunction (Table 3). Therefore, a more pronounced curvature as well as a longer distance of the cranial stent end to the VCI were found to be independent predictors of TIPS dysfunction.

To address the issue of differing time points for CT scans after TIPS insertion used in assessing 3D TIPS geometry, we conducted an additional analysis that considered the time from TIPS insertion to CT acquisition. In the univariate analysis, a significant association was observed between the time from TIPS insertion to CT acquisition and TIPS dysfunction ($p=0.027$, HR 0.999, 95% CI 0.998–1.000). However, it is worth noting that in the multivariate analysis, the only parameters found to be associated with TIPS dysfunction were once again 3D stent curvature ($p=0.004$, HR 1.020, 95% CI 1.007–1.034) and 3D cranial TIPS stent end ($p<0.001$, HR 1.055, 95% CI 1.025–1.087) (Table 4).

3.4 | Predictors of Overt HE

To investigate risk factors for the development of overt hepatic encephalopathy (HE) following TIPS insertion, we performed an additional Cox regression analysis with overt HE as the endpoint. This analysis included the parameters previously identified as being associated with TIPS dysfunction. In the univariate model, the 3D cranial TIPS stent end was significantly inversely associated with the development of overt HE ($p=0.024$, HR 0.973, 95% CI 0.950–0.996). In contrast, 3D stent curvature was not significantly associated with the development of overt HE following TIPS insertion in the univariate analysis ($p=0.132$, HR 0.983, 95% CI 0.961–1.005) (Table S2).

3.5 | Subgroup Analysis—TIPS for Ascites

Additionally, a subgroup analysis was conducted in patients receiving TIPS for refractory ascites. Detection of ascites more than 30 days after TIPS insertion was the endpoint. Of the 60 patients, 19 (31.7%) ascites could be detected more than 30 days after TIPS insertion at a median time of 48 days. However, although 21 patients (35%) received invasive TIPS revision, ascites could only be detected in 11 patients (18.3%) before TIPS revision. Interestingly, none of the parameters were found to be significantly associated with the detectability of ascites at least 30 days after TIPS insertion (Table S3).

4 | Discussion

This study demonstrates for the first time that a semiautomated assessment of 3D TIPS geometry can predict TIPS dysfunction and the need for revision. In our study, two parameters were linked to the development of TIPS dysfunction. First, a longer distance of the cranial stent end to the IVC. This result is in line

TABLE 1 | Study population characteristics at baseline.

Parameter	All (n = 107)	No dysfunction (n = 75)	TIPS dysfunction (n = 32)	p
General characteristics				
Age (years)	58 (51–65)	58 (51–65)	58 (51–64)	0.911
Sex (male/female)	57/50 (53.3%/46.7%)	42/33 (56%/44%)	15/17 (46.9%/53.1%)	0.386
TIPS indication (variceal bleeding/ refractory ascites/other)	37/60/10 (34.6%/56.15/9.3%)	27/29/9 (36%/52%/12%)	10/21/1 (31.3%/65.6%/3.1)	0.249
Aetiology of cirrhosis (alcohol related/other)	63/44 (58.9%/41.1%)	44/31 (58.67%/41.33%)	19/13 (59.38%/40.62%)	0.946
Medical history				
Ascites (yes)	81 (76.41%)	57 (77.03%)	24 (75%)	0.821
Variceal bleeding (yes)	45 (42.45%)	33 (44.59%)	12 (37.5%)	0.498
Overt hepatic encephalopathy (yes)	17 (16.19%)	14 (18.67%)	3 (10.0%)	0.276
Oesophageal varices grade (no/1/2/3/4)	9/29/38/18/2 (9.38%/30.2% /39.58%/18.75%/2.08%)	6/19/28/14/1 (8.82%/27.94%/41.18%/20.59%/ 1.47%)	3/10/10/4/1 (10.71%/35.71 %/35.71%/14.29%/3.57%)	0.833
Scores				
MELD	10 (8–13)	10 (8–14)	10.5 (8–12)	0.509
MELD-Na	21 (20–23)	21 (20–24)	21.5 (20–23)	0.579
Child–Pugh score	9 (7–10)	9 (8–10)	8 (7–9.75)	0.257
Child–Pugh grade (A/B/C)	14/61/32 (13.1%/57%/29.9%)	8/43/24 (10.7%/57.3%/32%)	6/18/8 (18.8%/56.3%/25%)	0.474
Hepatic haemodynamics				
CV-pressure before TIPS	6 (4–10)	7 (3–10.5)	6 (4–9.25)	0.705
PV-pressure before TIPS	26.5 (23–32)	26 (23–31.25)	27 (24–32.25)	0.548
PSPG before TIPS	20 (16–23)	20 (16–23.5)	20 (18–23)	0.779
CV-pressure after TIPS	9 (7–13)	9 (7–12)	11 (7–15.25)	0.250
PV-pressure after TIPS	19 (15–22)	19 (14.75–22)	20 (17–24.25)	0.294
PSPG after TIPS	8 (6–10.75)	8 (6.5–10.5)	7 (5–11)	0.599

Note: Categorical variables are presented in absolute cases and per cent while continuous variables are presented as median with interquartile range. Nonparametric testing (Qui-square test for categorical variables and Mann–Whitney U test for continuous variables).
Abbreviations: CV-pressure, central venous pressure (mmHg); MELD, model for end-stage liver disease; PSPG, portosystemic pressure gradient (mmHg); PV-pressure, portal venous pressure (mmHg); TIPS, Transjugular intrahepatic portosystemic shunt.

TABLE 2 | 3D TIPS geometry parameters obtained by CT and procedure data.

Parameter		All (n = 107)	No dysfunction (n = 75)	TIPS dysfunction (n = 32)	p
3D TIPS geometry	3D Cranial TIPS stent end (mm)	9.99 (2.00–17.93)	6.00 (1.97–14.12)	16.49 (12.24–26.51)	<0.001
	3D Minimal stent diameter (mm)	8.27 (7.71–9.01)	8.24 (7.66–9.05)	8.32 (7.73–8.87)	0.996
	3D Length of covered stent portion (mm)	63.03 (55.01–72.00)	66.02 (58.03–72.97)	55.45 (47.98–69.28)	0.001
	3D Stent curvature (degrees)	42.12 (36.47–50.37)	40.68 (35.67–49.96)	47.21 (41.30–54.94)	0.017
	3D Angle between the covered stent ends (degrees)	81.60 (66.88–98.73)	81.96 (66.61–102.9)	80.52 (66.89–92.51)	0.414
	3D α Angle (degrees)	53.71 (40.64–64.92)	51.86 (42.36–62.61)	58.48 (39.81–69.5)	0.406
	3D Confluence to TIPS stent (mm)	60.02 (48.02–77.04)	57.94 (46.94–75.08)	66.50 (53.80–80.44)	0.058
Procedure data	Nominal stent length (cm)	7 (6–8)	8 (7–8)	6 (6–8)	0.004
	Nominal stent diameter (mm)	10 (10–10)	10 (10–10)	10 (10–10)	0.116
	Stent dilatation after TIPS procedure (mm)	8 (8–8)	8 (8–8)	8 (8–8)	0.218
	Underdilated TIPS	90 (86.5%)	66 (89.2%)	24 (80.0%)	0.214
	Type of stent (VTS/VCX)	61/46 (57%/43%)	41/34 (54.7%/45.3%)	20/12 (62.5%/37.5%)	0.454

Note: Categorical variables are presented in absolute cases and per cent, while continuous variables are presented as median with interquartile range. Nonparametric testing (Qui-square test for categorical variables and Mann–Whitney U test for continuous variables). 3D cranial TIPS stent end (mm): Length from the cranial TIPS stent end in the liver vein to the IVC; 3D minimal stent diameter (mm): Smallest diameter in the entire TIPS stent; 3D Length of covered stent portion (mm): Length from the beginning of the distal covered stent end to the end of the cranial covered stent end; 3D stent curvature (degrees/cm): Result of segmentation of the path within the TIPS stent into straight lines with gaps of 5 mm and angle measurements over 1 cm. The parameter describes the maximum change in direction between these sections within the entire stent; 3D angle between the covered stent ends (degrees): Angle between two straight lines orthogonal to the covered stent ends; 3D α angle (degrees): Angle formed between the beginning of the covered stent in the PV and the course of the PV; 3D confluence to TIPS stent (mm): Length from the beginning of the path to the beginning of the uncovered distal stent end.

Abbreviations: TIPS, transjugular intrahepatic portosystemic shunt; VCX, VIATORR controlled expansion stent; VTS: VIATORR TIPS stent.

with our and other previous publications on 2D TIPS geometry [18] and relevant for clinical practice because the cranial stent end position can be influenced by the interventionalist's choice of a stent with an adequate length and positioning of the stent. Secondly, and as the key novel finding of our study, we identified a more pronounced curvature as linked to the development of TIPS dysfunction. In this regard, we suggest inserting the TIPS more centrally to avoid a larger curvature of the stent and consecutive potentially problematic haemodynamics of the stent, which might be associated with the development of TIPS dysfunction.

In recent years, several studies evaluated predictors of TIPS dysfunction that are related to TIPS geometry and position. However, the methodology in the current literature is inhomogeneous. Some studies evaluated two-dimensional imaging such as angiograms, while few others evaluated CT scans. Therefore, the proposed predictors are diverse, including the use of bare metal compared to covered stents, interventionalist's experience [16] and portal venous flow post TIPS [17] as well as α angle or stent position [24, 25]. Except for the use of bare metal stents

compared to covered stents, generally, validation for these proposed parameters as predictors of TIPS dysfunction is lacking [10, 12, 14].

Our study depicts the predictive value of 3D TIPS geometry parameters. The analysis of 3D imaging might be more suited to adequately represent the complex anatomy than the analysis of 2D angiography images. A major limitation of the analysis of 2D images is the insufficient representation of the complex portal venous and hepatic anatomy [26]. An optimal 2D angiography angle for TIPS projection is not consented. In a study, the mean optimal projection view for TIPS stent placement was 27° right oblique and 3°craniocaudal. However, even this optimal projection angle showed poor intra- and interobserver variability of only 0.6 and 0.48, respectively [27].

Apart from the heterogeneous imaging modalities to evaluate the impact of TIPS geometry on TIPS dysfunction, measuring those parameters (angles, lengths, distance to IVC, etc.) requires time-consuming manual labour from a trained healthcare specialist. While algorithm-based automated image analysis is

TABLE 3 | Uni- and multivariate Cox regression analysis. Endpoint: TIPS dysfunction.

Parameter		<i>p</i>	Univariate HR	95% CI	<i>p</i>	Multivariate HR	95% CI
3D CT evaluation	3D Cranial TIPS stent end (mm)	<0.001	1.057	1.026–1.090	<0.001	1.061	1.030–1.093
	3D Minimal stent diameter (mm)	0.352	0.797	0.495–1.285			
	3D Length of covered stent portion	0.066	0.967	0.934–1.002			
	3D Stent curvature (degrees)	0.002	1.019	1.007–1.032	0.003	1.020	1.007–1.034
	3D Angle between the covered stent ends (degrees)	0.334	0.992	0.977–1.008			
	3D α Angle (degrees)	0.763	1.003	0.984–1.022			
	3D Confluence to TIPS stent (mm)	0.375	1.007	0.991–1.024			
Procedure data	Nominal stent length (cm)	0.062	0.741	0.541–1.016			
	Nominal stent diameter (mm)	0.199	0.517	0.189–1.414			
	Stent dilatation after TIPS procedure (mm)	0.145	1.437	0.882–2.340			
	Underdilated TIPS (yes)	0.069	0.429	0.173–1.069			
Scores	Child–Pugh Score before TIPS	0.627	0.950	0.773–1.168			
	MELD before TIPS	0.917	0.995	0.901–1.098			
Hepatic haemodynamics	CV pressure before TIPS (mmHg)	0.721	0.984	0.902–1.074			
	PV pressure before TIPS (mmHg)	0.888	1.005	0.944–1.069			
	PSPG before TIPS (mmHg)	0.592	1.018	0.955–1.084			
	CV pressure after TIPS (mmHg)	0.850	0.992	0.917–1.074			
	PV pressure after TIPS (mmHg)	0.353	1.035	0.962–1.113			
	PSPG after TIPS (mmHg)	0.119	1.070	0.983–1.165			

Note: 3D cranial TIPS stent end (mm) Length from the cranial TIPS stent end in the liver vein to the IVC; 3D Minimal stent diameter (mm): Smallest diameter in the entire TIPS stent; 3D Length of covered stent portion (mm): Length from the beginning of the distal covered stent end to the end of the cranial covered stent end; 3D stent curvature (degrees/cm): Result of segmentation of the path within the TIPS stent into straight lines with gaps of 5 mm and angle measurements over 1 cm. The parameter describes the maximum change in direction between these sections within the entire stent; 3D angle between the covered stent ends (degrees): Angle between two straight lines orthogonal to the covered stent ends; 3D α angle (degrees): Angle formed between the beginning of the covered stent in the PV to the course of the PV; 3D confluence to TIPS stent (mm): Length from the beginning of the path to the beginning of the uncovered distal stent end.

Abbreviations: CI, confidence interval; CV, central venous; HR, hazard ratio; MELD, model for end-stage liver disease; PSPG, portosystemic pressure gradient; PV, portal venous; TIPS, transjugular intrahepatic portosystemic shunt.

being intensively studied in other areas of liver cirrhosis, such as in the automated assessment of sarcopenia [7, 28, 29] or spontaneous portosystemic shunts [30, 31], there are currently no

studies evaluating the computer-assisted, (semi-)automated assessment of TIPS geometry. This study demonstrates a modern approach and shows the predictive value of 3D TIPS geometry

TABLE 4 | Additional uni- and multivariate Cox regression analyses including the significant parameters of the multivariate analysis of Table 3 and time from TIPS insertion to CT acquisition. Endpoint: TIPS dysfunction.

Parameter	<i>p</i>	Univariate HR	95% CI	<i>p</i>	Multivariate HR	95% CI
3D Cranial TIPS stent end (mm)	<0.001	1.057	1.026–1.090	<0.001	1.055	1.025–1.087
3D Stent curvature (degrees)	0.002	1.019	1.007–1.032	0.004	1.020	1.007–1.034
Time from TIPS insertion to CT acquisition	0.027	0.999	0.998–1.000			

Note: 3D cranial TIPS stent end (mm): Length from the cranial TIPS stent end in the liver vein to the IVC; 3D stent curvature (degrees/cm): Result of segmentation of the path within the TIPS stent into straight lines with gaps of 5 mm and angle measurements over 1 cm. The parameter describes the maximum change in direction between these sections within the entire stent.
Abbreviations: CI, confidence interval; HR, hazard ratio; TIPS, transjugular intrahepatic portosystemic shunt.

for the first time. With our algorithm, it is potentially feasible for the clinician to evaluate 3D TIPS geometry in clinical practice in order to stratify patients at risk for TIPS dysfunction. However, we do not suggest routinely performing CT scans after TIPS insertion outside of routine clinical practice to evaluate TIPS geometry because this would mean the need for a second intervention with potential risk and cost factors. A more easily available alternative to facilitate 3D TIPS geometry measurements after TIPS insertion could be to perform routine cone beam CT at the end of the TIPS insertion procedure. However, this study was not intended to encourage routine measurements of 3D TIPS geometry postinsertion but rather to demonstrate the role of 3D geometry regarding the prediction of TIPS dysfunction. Instead of routinely assessing 3D TIPS geometry after insertion, we suggest taking the parameters that we were able to identify as risk factors for the development of TIPS dysfunction into consideration. In terms of the applicability of our data for routine clinical practice and as mentioned earlier, we suggest inserting the TIPS stent into a more central portal venous branch and choosing a stent that is long enough to reach the IVC junction to reduce the risk for TIPS dysfunction. However, one of the main complications that can occur after TIPS implantation is HE. Interestingly, in our separate analyses with overt HE after TIPS insertion as an endpoint, a shorter distance of the cranial TIPS stent end was associated with overt HE after TIPS insertion while the stent curvature was not significantly associated with overt HE after TIPS insertion. Thus, the optimal position of the cranial TIPS stent end regarding risk minimisation for both TIPS dysfunction as well as the development of overt HE after TIPS still has to be determined. Even though this is a comprehensive and so far unique approach and analysis, there are some limitations. The main limitation is the retrospective and monocentric character of the study limiting its generalisability as well as the small number of patients. Additionally, it is important to acknowledge that the stent grafts utilised in this study are a mix of VIATORR controlled expansion stent grafts (VCX) and VIATORR TIPS endoprosthesis stent grafts (VTS). VCX stents were introduced during the study's inclusion period, and the analysis includes both VTS and VCX stents. Notably, the distribution of these two types of stent grafts was similar between the TIPS dysfunction and nondysfunction groups. Therefore, we believe that the findings of our study remain relevant and applicable between the two stent types. Furthermore, we are not able to provide data on heart failure following TIPS implantation because this was not part of the routinely assessed data. The subgroup analysis of patients who received TIPS for refractory

ascites revealed no significant association of 3D TIPS geometry with detectable ascites at least 30 days following TIPS insertion. This finding may be attributable to the relatively small sample size within this subgroup. Overall, detectable ascites after TIPS insertion might not necessarily only be related to TIPS dysfunction and could potentially be multifactorial, for example, due to cardiac dysfunction or differences in terms of adherence to diuretic medication.

However, all studies on this topic suffer from a nonstandardised TIPS procedure performed across the world [32]. Mainly, the clinical practice of anticoagulation during and after the TIPS procedure is still debated, and no general consensus exists, despite this factor being potentially crucial for the development of TIPS dysfunction by in-stent thrombosis. Finally, our algorithm does not account for spontaneous portosystemic shunts (SPSS). SPSS redirect portal venous flow, and the total SPSS area (TSA) have been identified as a significant factor for the outcome of cirrhotic patients [30, 33]. In the context of TIPS, SPSS may function as a competing shunt impacting its function [34]. However, no significant impact on TIPS dysfunction was observed in a recent large cohort [35].

In conclusion, this study shows a modern approach of a computer-assisted semiautomated assessment of 3D TIPS stent geometry demonstrating its predictive value for the development of TIPS dysfunction. Overall, we were able to identify a larger stent curvature as well as a larger distance of the cranial TIPS stent end to the IVC as risk factors for the development of TIPS dysfunction, both of which can potentially be addressed by clinical measures.

Author Contributions

Carsten Meyer: conceptualization, investigation, data curation, writing – review and editing, methodology, supervision. **Markus Kimmann:** conceptualization, investigation, formal analysis, writing – original draft, methodology, data curation, visualization, validation. **Katharina Böhm:** data curation, conceptualization, writing – original draft, investigation, methodology, formal analysis, validation, visualization. **Sebastian Nowak:** data curation, investigation, writing – review and editing. **Alba Maria Paar Pérez:** investigation, writing – review and editing, data curation. **Jörn Arne Meier:** investigation, writing – review and editing. **Sara Noemi Reinartz Groba:** investigation, writing – review and editing. **Juliana Gödiker:** investigation, writing – review and editing. **Frank Erhard Uschner:** investigation, writing – review and editing. **Feras Sanoubara:** investigation, writing –

review and editing. **Johannes Chang:** data curation, investigation, writing – review and editing. **Jonel Trebicka:** conceptualization, project administration, writing – review and editing, investigation. **Alois Martin Sprinkart:** methodology, conceptualization, investigation, supervision, data curation, resources, software, visualization, project administration. **Michael Praktijnjo:** conceptualization, investigation, data curation, supervision, methodology, writing – original draft, resources, funding acquisition, formal analysis, visualization, validation, project administration.

Acknowledgements

We thank Nadine Köstlmeier and Julia Groffy for their excellent technical assistance. Open Access funding enabled and organized by Projekt DEAL.

Ethics Statement

The ethical review board of the University Hospital of Bonn approved the study (positive ethical review board vote 038/20).

Consent

Written, informed consent was obtained from each patient included in the study.

Conflicts of Interest

The authors declare no conflicts of interest.

Data Availability Statement

The data that support the findings of this study are available from the corresponding author upon reasonable request.

Authors Statement

All authors approved the final version of the article, including the authorship list.

References

1. M. L. Volk, R. S. Tocco, J. Bazick, M. O. Rakoski, and A. S. Lok, “Hospital Re-Admissions Among Patients With Decompensated Cirrhosis,” *American Journal of Gastroenterology* 107 (2012): 247–252.
2. M. Rössle, “TIPS: 25 Years Later,” *Journal of Hepatology* 59 (2013): 1081–1093.
3. P. Angeli, M. Bernardi, C. Villanueva, et al., “EASL Clinical Practice Guidelines for the Management of Patients With Decompensated Cirrhosis [Internet],” *Journal of Hepatology* 69 (2018): 406–460.
4. J. C. García-Pagán, K. Caca, C. Bureau, et al., “Early Use of TIPS in Patients With Cirrhosis and Variceal Bleeding,” *New England Journal of Medicine* 362 (2010): 2370–2379.
5. C. Bureau, D. Thabut, F. Oberti, et al., “Transjugular Intrahepatic Portosystemic Shunts With Covered Stents Increase Transplant-Free Survival of Patients With Cirrhosis and Recurrent Ascites,” *Gastroenterology* 152 (2017): 157–163.
6. J. Trebicka, “Does Transjugular Intrahepatic Portosystemic Shunt Stent Differentially Improve Survival in a Subset of Cirrhotic Patients?,” *Seminars in Liver Disease* 38 (2018): 87–96.
7. M. Praktijnjo, M. Book, J. Luetkens, et al., “Fat-Free Muscle Mass in Magnetic Resonance Imaging Predicts Acute-On-Chronic Liver Failure and Survival in Decompensated Cirrhosis,” *Hepatology* Baltimore Md 67, no. 3 (2018): 1014–1026, <https://doi.org/10.1002/hep.29602>.

8. M. W. Russo, P. F. Jacques, M. Mauro, et al., “Predictors of Mortality and Stenosis After Transjugular Intrahepatic Portosystemic Shunt,” *Liver Transplantation* 8, no. 3 (2002): 271–277, <https://doi.org/10.1053/jlts.2002.31653>.
9. A. J. Sanyal, A. M. Freedman, V. A. Luketic, et al., “The Natural History of Portal Hypertension After Transjugular Intrahepatic Portosystemic Shunts,” *Gastroenterology* 112 (1997): 889–898.
10. C. Bureau, J. C. G. Pagan, G. P. Layrargues, et al., “Patency of Stents Covered With Polytetrafluoroethylene in Patients Treated by Transjugular Intrahepatic Portosystemic Shunts: Long-Term Results of a Randomized Multicentre Study,” *Liver International Official Journal of International Association Study Liver* 27, no. 6 (2007): 742–747, <https://doi.org/10.1111/j.1478-3231.2007.01522.x>.
11. M. Eesa and T. Clark, “Transjugular Intrahepatic Portosystemic Shunt: State of the Art,” *Seminars in Roentgenology* 46 (2011): 125–132.
12. B. Geeroms, W. Laleman, A. Laenen, et al., “Expanded Polytetrafluoroethylene-Covered Stent-Grafts for Transjugular Intrahepatic Portosystemic Shunts in Cirrhotic Patients: Long-Term Patency and Clinical Outcome Results,” *European Radiology* 27 (2017): 1795–1803.
13. F. He, S. Dai, Z. Xiao, et al., “Pathological Predictors of Shunt Stenosis and Hepatic Encephalopathy After Transjugular Intrahepatic Portosystemic Shunt,” *BioMed Research International* 2016 (2016): 3681731.
14. Y.-M. Wan, Y.-H. Li, Y. Xu, et al., “Predictors of Shunt Dysfunction and Overall Survival in Patients With Variceal Bleeding Treated With Transjugular Portosystemic Shunt Creation Using the Fluency Stent Graft,” *Academic Radiology* 25 (2018): 925–934.
15. S.-H. Luo, J.-G. Chu, H. Huang, and K. C. Yao, “Effect of Initial Stent Position on Patency of Transjugular Intrahepatic Portosystemic Shunt,” *World Journal of Gastroenterology* 23 (2017): 4779–4787.
16. M. Buechter, P. Manka, G. Gerken, et al., “Transjugular Intrahepatic Portosystemic Shunt in Patients With Portal Hypertension: Patency Depends on Coverage and Interventionalist’s Experience,” *Digestive Diseases Basel Switz* 36, no. 3 (2018): 218–227, <https://doi.org/10.1159/000486030>.
17. A. Chien, Y.-L. Wang, J. McWilliams, E. Lee, and S. Kee, “Venographic Analysis of Portal Flow After TIPS Predicts Future Shunt Revision,” *American Journal of Roentgenology* 211 (2018): 684–688.
18. C. Meyer, A. M. Paar Pérez, J. Chang, et al., “Cranial Stent Position Is Independently Associated With the Development of TIPS Dysfunction [Internet],” *Scientific Reports* 12 (2022): 3559.
19. J. Klasen-Sansone, J. Bode, R. S. Lanzman, et al., “TIPS Geometry Influences Patency,” *Zeitschrift für Gastroenterologie* 53 (2015): 28–32.
20. X. Wang, X. Luo, M. Zhao, J. Song, X. Li, and L. Yang, “Prognostic Factors for Acute Transjugular Intrahepatic Portosystemic Shunt Occlusion Using Expanded Polytetrafluoroethylene-Covered Stent,” *Digestive Diseases and Sciences* 65, no. 10 (2019): 3032–3039, <https://doi.org/10.1007/s10620-019-06008-4>.
21. M. Praktijnjo, C. Clees, A. Pigliacelli, et al., “Sarcopenia Is Associated With Development of Acute-On-Chronic Liver Failure in Decompensated Liver Cirrhosis Receiving Transjugular Intrahepatic Portosystemic Shunt,” *Clinical and Translational Gastroenterology* 10 (2019): e00025.
22. M. Praktijnjo, J. Lehmann, M. J. Nielsen, et al., “Acute Decompen-sation Boosts Hepatic Collagen Type III Deposition and Deteriorates Experimental and Human Cirrhosis,” *Hepatology Communications* 2 (2018): 211–222.
23. J. Lehmann, M. Praktijnjo, M. J. Nielsen, et al., “Collagen Type IV Remodelling Gender-Specifically Predicts Mortality in Decompensated Cirrhosis,” *Liver International Official Journal of International Association Study Liver* 39, no. 5 (2019): 885–893, <https://doi.org/10.1111/liv.14070>.

24. B. Andring, S. P. Kalva, P. Sutphin, et al., "Effect of Technical Parameters on Transjugular Intrahepatic Portosystemic Shunts Utilizing Stent Grafts," *World Journal of Gastroenterology* 21 (2015): 8110–8117.
25. P. J. Schaefer, T. Jahnke, F. K. Schaefer, et al., "Transjugular Intrahepatic Portosystemic Shunt: Evaluation of the Impact of the Stent's Configuration on the Patency Rate," *RoFo Fortschritte auf dem Gebiete der Rontgenstrahlen und der Nuklearmedizin* 179 (2007): 965–970.
26. J. P. Lee, "Variation in Portal and Hepatic Venous Anatomy as Shown by Magnetic Resonance Imaging: Implication for Transjugular Intrahepatic Portosystemic Shunt," *Clinical Radiology* 50 (1995): 108–110.
27. G. Maleux, X. Jiang, S. Heye, et al., "Transjugular Intrahepatic Portosystemic Shunt Stent-Graft Placement: Mean Optimal Portal Venous Projection View Determined by Three-Dimensional Portography," *Acta Radiologica Stockh. Sweden* 13, no. 54 (1987): 516–520.
28. J. A. Luetkens, A. Faron, H. L. Geissler, et al., "Opportunistic Computed Tomography Imaging for the Assessment of Fatty Muscle Fraction Predicts Outcome in Patients Undergoing Transcatheter Aortic Valve Replacement," *Circulation* 141 (2020): 234–236.
29. S. Nowak, A. Faron, J. A. Luetkens, et al., "Fully Automated Segmentation of Connective Tissue Compartments for CT-Based Body Composition Analysis: A Deep Learning Approach," *Investigative Radiology* 55 (2020): 357–366.
30. M. Praktijn, M. Simón-Talero, J. Römer, et al., "Total Area of Spontaneous Portosystemic Shunts Independently Predicts Hepatic Encephalopathy and Mortality in Liver Cirrhosis," *Journal of Hepatology* 72 (2020): 1140–1150.
31. M. Praktijn, J. Torner, M. Simón-Talero, et al., "Definition of SPSS: We Need to Speak the Same Language: Computer-Assisted Image Processing for Better Quantification," *Journal of Hepatology* 73 (2020): 464–465.
32. C. J. Steib, H. Li, J. Zhang, et al., "Transjugular Intrahepatic Portosystemic Shunt for Patients With Liver Cirrhosis: Survey Evaluating Indications, Standardization of Procedures and Anticoagulation in 43 German Hospitals," *European Journal of Gastroenterology & Hepatology* 32, no. 9 (2019): 1179–1185, <https://doi.org/10.1097/MEG.0000000000001628>.
33. M. Simón-Talero, D. Roccarina, J. Martínez, et al., "Association Between Portosystemic Shunts and Increased Complications and Mortality in Patients With Cirrhosis," *Gastroenterology* 154 (2018): 1694–1705.e4.
34. X. Leng, F. Zhang, M. Zhang, et al., "Comparison of Transjugular Intrahepatic Portosystemic Shunt for Treatment of Variceal Bleeding in Patients With Cirrhosis With or Without Spontaneous Portosystemic Shunt," *European Journal of Gastroenterology & Hepatology* 31 (2019): 853–858.
35. C. He, Y. Lv, Z. Wang, et al., "Association Between Non-Variceal Spontaneous Portosystemic Shunt and Outcomes After TIPS in Cirrhosis," *Digestive and Liver Disease Official Journal of Italian Society of Gastroenterology Italian Association Study Liver* 50, no. 12 (2018): 1315–1323, <https://doi.org/10.1016/j.dld.2018.05.022>.

Supporting Information

Additional supporting information can be found online in the Supporting Information section.